Characterization of a Dissociative Excited State in the Solid State: Photochemistry of Poly(methyl methacrylate). Photochemical Processes in Polymeric Systems. 5[†,1]

Amitava Gupta,* Ranty Liang, Fun Dow Tsay, and Jovan Moacanin

Energy and Materials Research Section, Jet Propulsion Laboratory, California Institute of Technology, Pasadena, California 91103. *Received March 27, 1980*

ABSTRACT: Quantum yields of principal photoprocesses on direct excitation of poly(methyl methacrylate) have been measured at 303 K in vacuo. Radicals formed on bond cleavage following excitation have been characterized by ESR spectroscopy. Product analyses have been carried out by GC, GC–MS, and FT IR spectroscopy. A mechanism of photodegradation with the following principal features has been proposed in order to interpret these data: (1) The ester side chain undergoes photolytic bond cleavage with unit efficiency and (2) most chain radicals decay through recombination with small radicals.

Introduction

Photodegradation of poly(alkyl acrylates) and poly(alkyl methacrylates) has been the subject of several detailed studies.[2–6] For poly(methyl methacryalte), PMMA quantitative rate data exists mainly for temperatures of 423 K and above, a temperature regime which is characterized by complete unzipping of the polymer chain following initiation of chain scission through photolysis. The initial process of electronic excitation has not been understood completely, since the lowest absorption band in PMMA has not been yet assigned to a specific electronic transition. MacCallum et al.[4,5] observed that the quantum yield of scission (and unzipping) processes depends on the weight of the polymer film being exposed to radiation in the temperature range 433–473 K, a result which may be interpreted in terms of some type of secondary photolysis or an energy-transfer process. Measurements of quantum yields of photoproduct formation at room temperature (25 ± 3 °C) were reported by Fox and others. These data indicate a high quantum efficiency of photolytic bond cleavage at the ester side chain, while the tertiary carbon radical $CH_2\dot{C}(CH_3)$ may be depleted either via rearrangement to the "propagating radical" or by combination with small radicals.

A comprehensive mechanism of photodegradation of PMMA is expected to incorporate the identity and quantum yields of primary processes following excitation and also a description of the processes which result in the eventual decay of the radicals generated through photoexcitation. Measurement of rates of primary photoprocesses in aliphatic esters is only infrequently available in the literature.[7–9] The first n–π^* singlet in simple esters has an extinction coefficient of 45–50 at the band maximum which occurs at 220–230 nm. Bond cleavage following excitation is quite efficient, but there is no information on the relative photoreactivity of the first excited singlet and the first triplet state.

The fate of radicals generated through the initial bond-cleavage process is more complex: a few representative processes for PMMA are illustrated in Scheme I. Although the tertiary carbon radical I is a key intermediate, it has not been definitely identified in the ESR spectrum of irradiated PMMA at room temperature.[10–13] Hence it is believed that process 6 is rapid at room temperature. ESR spectra on irradiated PMMA has a complex structure mainly characterized by the "nine-line spectrum"

Scheme I

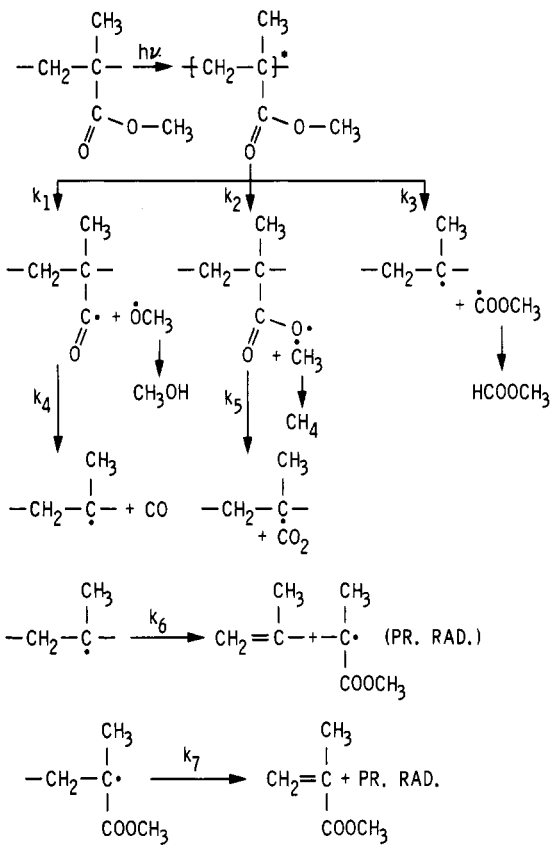

due to the propagating radical.[4] Methyl, acetyl, formyl, and formate radicals have also been identified in frozen samples (77 K).

In this paper, we report on the quantum yields of formation of photoproducts and chain scission as well as quantum yields of formation of the major radicals formed on bond cleavage. The rate of formation (or concentration) of various radicals has been plotted against radiation energy flux deposited at 77 K so that products of primary photolysis can be distinguished from those arising from secondary photolysis. Estimates of decay ratios of certain key radicals may be made by using the rate data so that the fraction of radicals decaying through recombination can be obtained.

Experimental Section

Poly(methyl methacrylate) [$\bar{M} \simeq (4–8) \times 10^5$] was obtained by free-radical polymerization and also by thermal polymerization of methyl methacrylate. 2,2′-Azobis(isobutyronitrile) was used

[†]This paper represents one phase of research performed at the Jet Propulsion Laboratory, California Institute of Technology, and sponsored by the Department of Energy by agreement with the National Aeronautics and Space Administration.

0024-9297/80/2213-1696$01.00/0

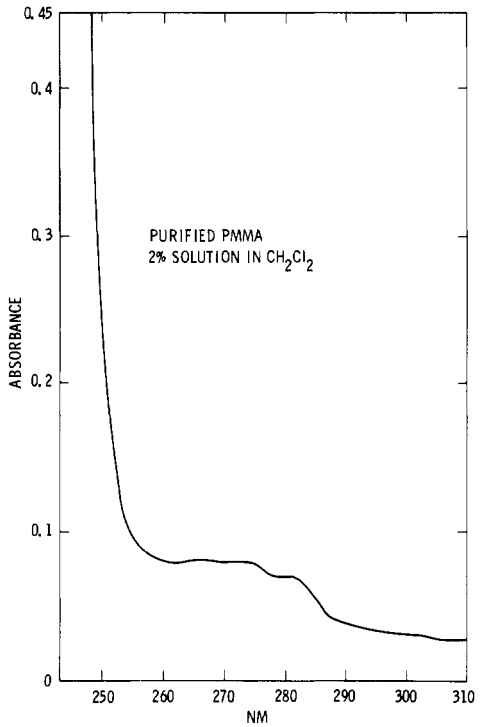

Figure 1. Absorption spectrum of PMMA in fluid solution. The extinction coefficient at 270 nm, calculated assuming infinite chain length (i.e., no end-group absorption), is approximately 0.2 L mol^{-1} cm^{-1}.

as the initiator in these runs. The polymer was purified by repeated reprecipitations and extraction with methanol. It exhibited a single molecular weight peak in the high-performance liquid chromatogram and its IR spectrum matched spectra available in the literature.

Two sources of radiation were used in this study: (a) light from a low-pressure Hg arc, >99% of the flux occurring at 2537 Å, and (b) a pulsed laser beam at 266 nm, used to irradiate samples at 77 K. PMMA films [(5–10) × 10^{-3} cm in thickness] were cast from spectroquality CH_2Cl_2 and were always pumped overnight immediately prior to being placed in a quartz tube and sealing off under vacuum. Subsequent to exposure, solvent was introduced through a break seal, the polymer was completely dissolved, and the solution was chilled at −10 °C for 1 h before the tube was opened and the solution analyzed. Product analysis was carried out by GC, GC–MS, and high-performance LC. The latter was also used to measure changes in molecular weight of the sample. Actinometry was performed with an *o*-nitrobenzaldehyde actinometer[14,15] and also by carrying out spectroradiometric measurements. Samples were also irradiated in sealed ESR tubes at 77 K and then transferred to the ESR cavity for measurement at 77 K. Radical concentrations were measured as a function of the number of pulses used. Samples were then thawed (300 K) and the radical concentration was measured again.

Results

Figure 1 shows an absorption spectrum of PMMA. Rates of formation of methanol and methyl formate are plotted as function of irradiation period in Figure 2. The linear plots indicate that competitive absorption arising from photoproducts is not significant in these runs. For higher conversions, strong deviations from linear behavior were always found, the average yields becoming smaller at higher conversions. Figure 3 shows the corresponding plot for chain scission, measured on the same films. The molecular weight data obtained by using polystyrene calibration curves were treated by the usual method, i.e., $\bar{M}_n^0/\bar{M}_n^t - 1 = \phi_{cs}I_1 = \phi_{cs}Itc_0$, where c_0 is the number of polymer chains present initially and I is the intensity of absorbed light. For good results absorbance of the film

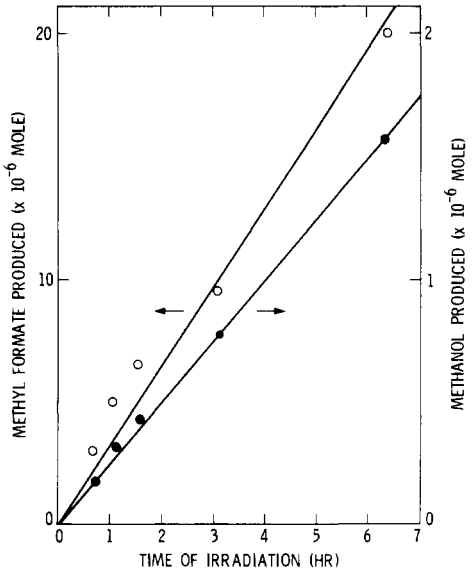

Figure 2. Methanol and methyl formate formation as a function of exposure period, measured on a gas chromatograph (20 ft × $^1/_8$ in., Poropak Q, FID).

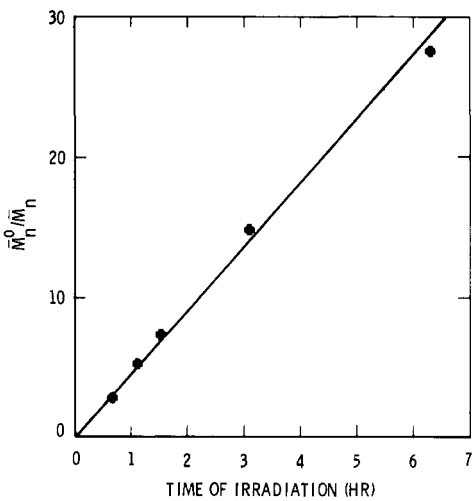

Figure 3. Plot of $\bar{M}_n^0/\bar{M}_n$ as a function of exposure period. Quantum yield of chain scission was calculated from the slope, using the equation $\bar{M}_n^0/\bar{M}_n - 1 = \phi_{cs}Itc_0$, where c_0 is the initial number of chains in the film being exposed.

should be kept low and was maintained at ≤0.1 in our experiments. It is also necessary to uniformly irradiate the whole film. A typical ESR spectrum after a few laser pulses is shown in Figure 4a. The signal is quite weak, and no significant measurements could be made at irradiation levels of fewer than 10 pulses (1 pulse is approximately equivalent to 1.6 × 10^{15} photons absorbed). Figure 4b shows signals due to radicals accumulated after 150 pulses, and Figure 4c shows the typical nine-line spectrum obtained on warming the sample to 300 K. Spectral simulation was used to identify and quantitate ·CHO, $\cdot CH_3CO$, $\cdot CH_3$, and $\cdot COOCH_3$ as well as the propagating radical in the composite spectrum (Figure 4). Table I gives the quantum yields of various species and photoproducts. The yield of the propagating radical was calculated from the spectrum of the thawed sample. The yield of the propagating radical at room temperature is much less, possibly because recombination with small radicals is more efficient at room temperature. Schnabel et al.[17] measured the rate of molecular weight decrease in a fluid solution of PMMA following excitation by a 2-μs pulse of 15-MeV electrons. They observed two mechanisms of chain scission corre-

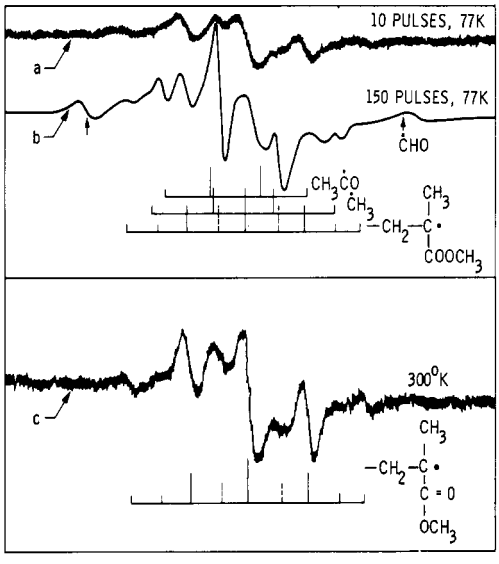

Figure 4. ESR spectra of solid polymer films irradiated with a 265-nm laser beam at 77 K: (a) spectrum recorded at 77 K after 10 pulses; (b) spectrum recorded at 77 K after 150 pulses; (c) spectrum recorded when sample was thawed to 300 K and then cooled back to 77 K.

Table I
Quantum Yield Data

photoproduct or photoprocess	quantum yield
CH_3OH	0.06[a,b] (10%)
$HCOOCH_3$	0.92[a] (10%)
methyl radical	0.083[b]
propagating radical	0.048[b]
propagating radical	0.014[c]
chain scission	0.05[a] (10%)
monomer	0.01[a] (20%)
formate radical	0.70[b]
formyl radical	0.012[b,d]
acetyl radical	0.044[b,d]

[a] PMMA films irradiated at 2537 Å under high vacuum at 25 °C. [b] PMMA films irradiated with the fourth harmonic of Nd-Yag laser (266 nm) at 77 K under vacuum; ESR spectra recorded on frozen samples. [c] Room temperature. [d] Average for 150 pulses.

Table II
ESR Parameters of Radicals Generated in Laser-Irradiated PMMA

radical	g values	proton hyperfine coupling constants, G
ĊHO	2.003 ± 0.001	126.0 ± 2.0
$\dot{C}H_3$	2.004 ± 0.001	23.0 ± 1.0
$CH_3\dot{C}O$	2.006 ± 0.001	18.0 ± 1.0
$-CH_2-\dot{C}(CH_3)COOCH_3$	2.004 ± 0.001	22.6 ± 1.0

sponding to two different rates, one fast (half-life approximately 20 μs) and the other relatively slow (half-life approximately 3 ms). It is possible to ascribe these two rates to processes 6 and 7, respectively, in Scheme I. Table II gives the g values and hyperfine coupling constants of the various radicals found in PMMA, in approximate agreement with literature. Figure 5 shows the rate of formation of the propagating radical as a function of the number of pulses incident on the sample. This graph has three regions, a linear region, a nonlinear region, and a

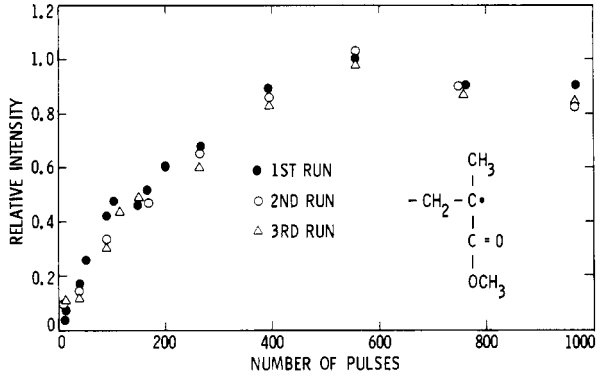

Figure 5. Relative intensity plots of radical concentrations at 77 K following exposure to a given number of laser pulses. All intensities are relative; spectral simulation was carried out subsequently in order to calculate quantum yields of radical generation reported in Table I.

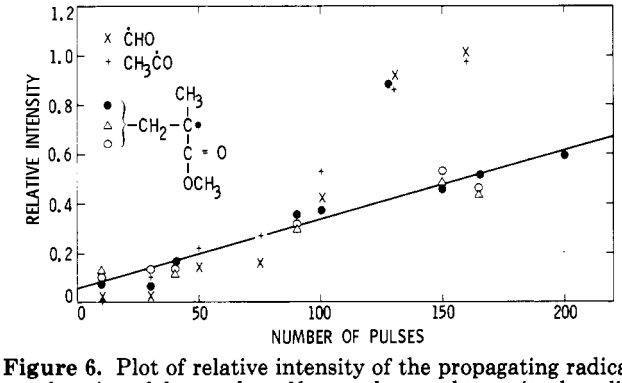

Figure 6. Plot of relative intensity of the propagating radical as a function of the number of laser pulses used to excite the solid films at 77 K.

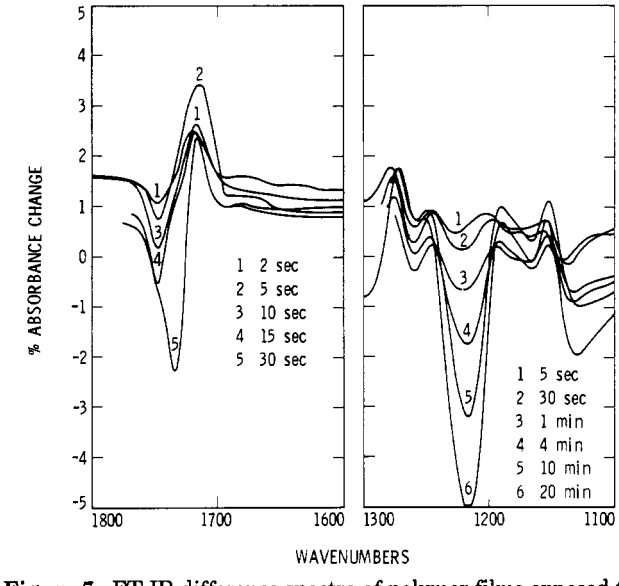

Figure 7. FT IR difference spectra of polymer films exposed to light from a medium-pressure Hg arc. The film was placed between two NaCl disks which were clamped together loosely and then placed in a sample holder equipped with a quartz window. The holder was purged with high-purity N_2 before irradiation and disassembled inside the N_2-purged sample compartment of the spectrometer, so that the sample was never exposed to air subsequent to the first exposure.

region where the radical concentration reaches an asymptotic value. Figure 6 shows plots of concentration of $\cdot CH_3CO$, $\cdot CHO$, and the propagating radical vs. the number of pulses incident on the sample. Figure 7 shows some FT IR spectroscopic data on irradiated PMMA films. These

Scheme II

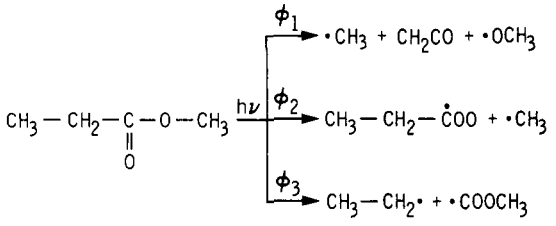

films were ultrathin (≤1 μm) and were directly deposited on a NaCl window prior to irradiation in a nitrogen atmosphere. Actinometry could not be performed under these conditions since a precise evaluation of the radiation energy absorbed by the PMMA film could not be made. The difference spectra indicate that for very short exposure periods a carbonyl peak grows in at 1705 cm^{-1} which decreases in intensity on longer exposure, but there is no significant increase in absorption in the 1200-cm^{-1} region, which corresponds to the ester C–O stretch. The ester side-chain groups undergo photolytic cleavage during the same time, as shown by a systematic decrease in intensities of the C=O stretch (1720 cm^{-1}) and C–O stretch (1215 cm^{-1}).

Discussion

The absorption coefficient of the solid film at 2537 Å, 5.6 cm^{-1}, is in approximate agreement with that reported by MacCallum.[5] The long-wavelength peak may be realistically assigned to the first triplet,[16] since the first excited (n–π*) singlet is expected to occur at 220–230 nm, and have a higher extinction coefficient (≥40). It may also be due to end-group absorption, although no molecular weight dependence could be detected on the extinction coefficient of the tail absorption (Figure 1). This assignment may be further tested by performing spectroscopy in the presence of a solvent containing heavy atoms, e.g., CH_2Br_2 or bromocyclopropane.

The most important conclusion which can be drawn from the quantum yield data is that

$$\phi_{\cdot CH_3} + \phi_{CH_3OH} + \phi_{HCOOCH_3} \simeq 1.0 \pm 0.1 \qquad (1)$$

This equation indicates that the excited state of PMMA is dissociative and undergoes bond cleavage with unit efficiency. This result shows that the unique photostability of PMMA to solar irradiance at ground level is due to the fact the PMMA absorbs very little, if any, of AM 1 solar irradiance.

The relative quantum yields of CH_3OH and $HCOOCH_3$ (and of $\cdot CH_3$ and $\cdot COOCH_3$) indicate that process k_3 is the most efficient bond-cleavage process. This result differs quite dramatically from data on simple esters such as methyl acetate and methyl propionate,[7-9] which indicate that, while bond-cleavage processes are indeed efficient, the cleavage mainly results in the formation of methoxy radicals and hence methanol is the major product. For example, in methyl propionate $\phi_1/(\phi_2 + \phi_3)$ is 4.2 at 34 °C, when ϕ_1, ϕ_2, and ϕ_3 are defined as quantum yields of the processes described in Scheme II. Dissociation from the excited state is believed to be also fully efficient in phenyl acetate, and the reactive excited state has been identified as the first (n–π*) singlet.[18]

The quantum yield of chain scission and the formation of propagating radical is very low compared with the yield of primary photoproducts. This results warrants the conclusion that most chain radicals (e.g., I) decay via recombination with small radicals on photolysis at room temperature. That this recombination is also quite efficient at 77 K is indicated by the appearance of signals due to ·CHO and $\cdot CH_3CO$ at about 50 pulses (Figure 6). Equations 2 and 3 may be used to illustrate the formation of precursors of these radicals in the system.

Table III
Comparison of Data from Fox et al.[2] and This Work

	photoproduct	quantum yield
this study	monomer	0.01
	scission	0.05
Fox et al.	monomer	0.20
	scission	0.04

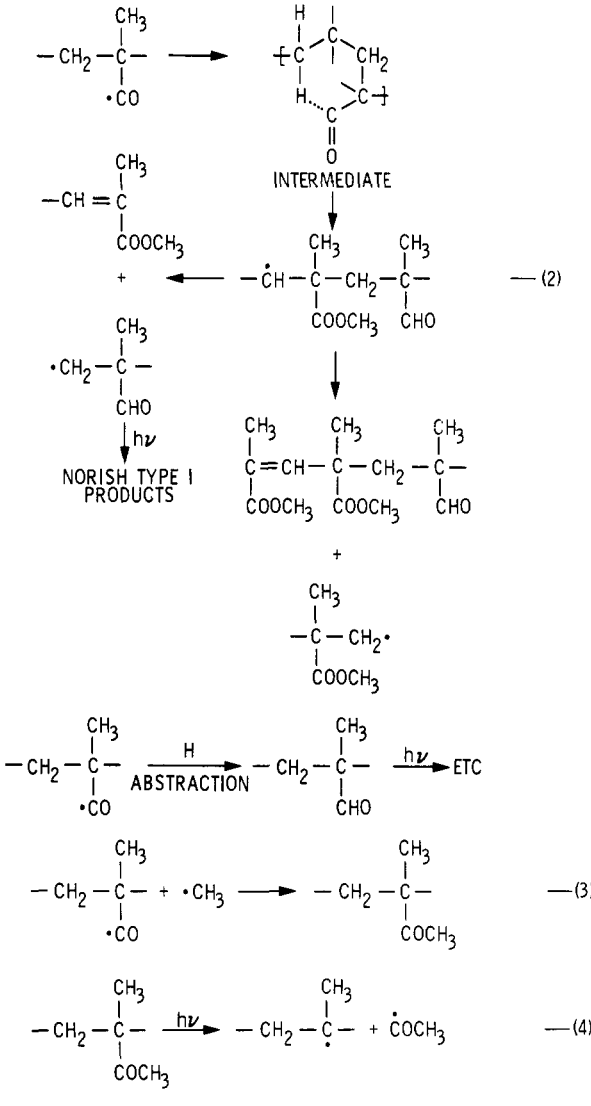

The plot in Figure 6 clearly demonstrates that $\cdot COCH_3$ and ·CHO are formed via secondary photolysis. FT IR spectra (Figure 7) also indicate formation of carbonyl groups for short exposure periods since we find an increase in absorption at 1705 cm^{-1} but no significant increase in the absorption in the 1100–1200-cm^{-1} region after 2–5 seconds of exposure. On longer exposure secondary photolysis takes place (eq 3 and 4) and the concentrations of aldehyde and ketonic groups reach a photostationary equilibrium. However, side-chain degradation soon reaches a point at which monitoring of these carbonyl groups is not possible by difference IR spectroscopy. The concentration profile of the propagating radical (Figure 5) reflects enhanced recombination processes such as eq 3, but the asymptotic behavior of this graph at high pulse rates strongly indicates that secondary photolysis of the propagating radical further reduces its concentration. Several

photochemical processes may be postulated as in eq 5 and 6. Intriguing support for process represented by eq 5

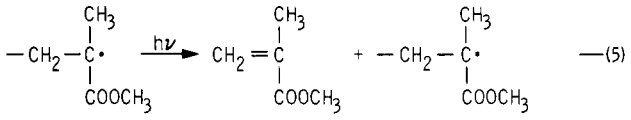

—(5)

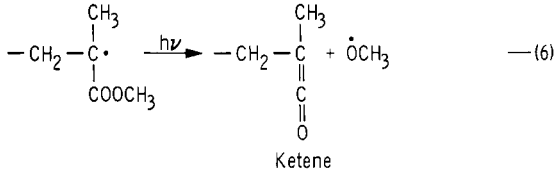

—(6)

Ketene

comes from a comparison of Fox's[2] data with ours. This is given in Table III. The quantum yields of chain scission are comparable, but the quantum yield of monomer formation is only about 0.01 in our study, while Fox et al. found this quantity to be 0.20. In other words, while we find approximately 0.2 unzipping steps per chain radical (i.e., approximately 80% of the chain radicals decay without forming any monomer), Fox found that there were approximately five unzipping processes per chain radical created by chain scission. It is noteworthy that a relatively broad-band source was used by Fox et al. which could induce considerable long-wavelength (250–250 nm) absorption by the propagating radical and induce unzipping via eq 5. Rates of some of these proposed abstraction processes (eq 2) may be significantly affected by the tacticity of the polymer chain. There is evidence that rates of degradation induced by exposure to an electron beam[19] and ultraviolet radiation[20] is significantly affected by the isomeric form in poly(methyl methacrylate). Henry and Gardener[20] observed that the rates of photodegradation of the isotactic and syndiotactic forms are significantly different. Their results also indicated that the number of bond breaks per gram of mixture of isomers was considerably less than what would be expected if each isomeric form was degrading independently. Our current work on this system involves an attempt to establish an unequivocal assignment of the lowest excited state of poly(methyl methacrylate) and study of the wavelength dependence of the quantum yields of various primary processes.

Acknowledgment. Numerous discussions with W. F. Carroll and S. Di Stefano are gratefully acknowledged. Lois Taylor and Ray Haack are acknowledged for analytical support. This research was jointly supported by the Low Cost Solar Array Project and the Materials Research and Technology Task sponsored by SERI/DOE.

References and Notes

(1) Gupta, A.; Liang, R.; Moacanin, J.; Kliger, D.; Horowitz, J.; Goldbeck, D.; Miskowski, V., part 4, submitted for publication.
(2) Fox, R. B.; Isaacs, L. G.; Stokes, S. *J. Polym. Sci., Part A* **1963**, *1*, 1079. Frolova, M. I.; Efimov, L. I.; Riabov, A. V. *Khim. Khim. Teknol.* **1964**, *7*, 304.
(3) Cowley, P. R. E. J.; Melville, H. W. *Proc. R. Soc. London, Ser. A* **1952**, *211*, 320. Charlesby, A.; Thomas, D. K. *Ibid.* **1962**, *269*, 104.
(4) Grassie, N. *Pure Appl. Chem.* **1973**, *34*, 247. Grassie, N.; Torrance, B. J. D.; Colford, J. G. *J. Polym. Sci., Part A-1* **1969**, *7*, 1425.
(5) MacCallum, J. R.; Schoff, C. F. *Trans. Faraday Soc.* **1971**, *67*, 2372, 2383.
(6) Morimoto, K.; Suzuki, S. *J. Appl. Polym. Sci.* **1972**, *16*, 2947.
(7) Calvert, J. G.; Pitts, J., Jr. "Photochemistry"; Wiley: New York, 1966; p 436.
(8) Ausloos, P. *Can. J. Chem.* **1958**, *36*, 383. *J. Am. Chem. Soc.* **1958**, *80*, 1310.
(9) Wijnen, M. H. J. *J. Chem. Phys.* **1958**, *28*, 271, 939.
(10) Kato, Y.; Nichioka, A. *Rep. Prog. Polym. Phys. Jpn.* **1966**, *9*, 477.
(11) Wong, P. K. *Polymer* **1974**, *15*, 60. Michel, R. E.; Chapman, F. W.; Mao, T. J. *J. Polym. Sci., Part A-1* **1967**, *5*, 677.
(12) Campbell, D. *Macromol. Rev.* **1970**, *4*, 91.
(13) Iwasaki, M.; Sakori, Y. *J. Polym. Sci., Part A-1* **1969**, *7*, 1537 and references therein.
(14) Gupta, A.; Yavrouian, A.; Di Stefano, S.; Merritt, C. D.; Scott, G. W. *Macromolecules* **1980**, *13*, 821.
(15) Cowell, G. W.; Pitts, J. N., Jr. *J. Am. Chem. Soc.* **1968**, *90*, 1106.
(16) Braun, D.; Berger, J. *Kolloid Z.* **1972**, *250*, 142. *Ibid.* **1971**, *248*, 871.
(17) Beck, G.; Lindenan, D.; Schnabel, W. *Macromolecules* **1977**, *10*, 135.
(18) Meyer, J. W.; Hammond, G. S. *J. Am. Chem. Soc.* **1972**, *94*, 2219.
(19) Gardner, D. G.; Henry, G. A.; Ward, D. "Energy Transfer in Radiation Processes"; Phillips, G., Ed.; Elsevier: Amsterdam, 1966; p 37.
(20) Gardner, D. G.; Henry, G. A. *J. Polym. Sci., Part B* **1967**, *5*, 101.

Polymerization of Trioxane Initiated by Isomeric 2,4,5-Trisubstituted 1,3-Dioxolan-2-ylium Salts

Zbigniew Jedliński* and Mirosław Gibas

Department of Polymer Chemistry, Technical University, Institute Gliwice of Polymer Chemistry, Polish Academy of Sciences, Zabrze, Poland. *Received March 27, 1980*

ABSTRACT: Polymerization of trioxane initiated by isomeric 2,4,5-trisubstituted 1,3-dioxolan-2-ylium hexafluoroarsenates was studied. The initiation was found to proceed by cationation. The influence of initiator nature on the rate of polymerization is discussed.

The polymerization rate of some unsaturated derivatives of 2,4,5-trisubstituted 1,3-dioxolane (1) was found to depend on the type and configuration of the substituents.[1] However, saturated analogues of 1 do not polymerize at all, although they react with triphenylmethylium salts, e.g., Ph_3CSbCl_6, to yield stable products.[2] We stated previously[3] that these products, i.e., the isomeric 2,4,5-trisubstituted 1,3-dioxolan-2-ylium hexachloroantimonates, exhibited a catalytic activity toward the trioxane monomer, whereby the course of polymerization depended distinctly on the structure of the trisubstituted 1,3-dioxolan-2-ylium cation.

0024-9297/80/2213-1700$01.00/0